Trapped ion mobility spectrometry time-of-flight mass spectrometry for high throughput and high resolution characterization of human milk oligosaccharide isomers

Aurélie Delvaux, Estelle Rathahao-Paris, Blanche Guillon, Sophie Cholet, Karine Adel-Patient, François Fenaille, Christophe Junot, Sandra Alves

Trapped ion mobility spectrometry time-of-flight mass spectrometry for high throughput and high resolution characterization of human milk oligosaccharide isomers

Aurélie Delvaux[1], Estelle Rathahao-Paris[1,2*], Blanche Guillon[2], Sophie Cholet[2], Karine Adel-Patient[2], François Fenaille[2], Christophe Junot[2], Sandra Alves[1*]

[1] Sorbonne Université, Faculté des Sciences et de l'Ingénierie, Institut Parisien de Chimie Moléculaire (IPCM), 75005 Paris, France

[2] Université Paris-Saclay, CEA, INRAE, Département Médicaments et Technologies pour la Santé (DMTS), SPI, 91191 Gif-sur-Yvette, France

* Corresponding authors :

Dr. Sandra Alves
Sorbonne Université, Faculté des Sciences et de l'Ingénierie, Tour 42-43, 4ème étage, BP 45, 4 place Jussieu F-75005, Paris, FRANCE.
E-mail: sandra.alves@sorbonne-universite.fr
or
Dr. Estelle Rathahao-Paris
UMR CEA-INRAE Médicaments et Technologies pour la Santé, Laboratoire d'Immuno-Allergie Alimentaire, CEA de Saclay- Bat 136, F-91191, Gif-sur-Yvette cedex, FRANCE.
E-mail: estelle.paris@inrae.fr

Abstract:

The microbiome and immune system of infants are shaped by various bioactive components of human breastmilk, notably human milk oligosaccharides (HMOs). HMOs represent the third component of breastmilk and exhibit extremely high structural diversity with many isomers. Here, we propose a high throughput and high resolution approach to characterize main oligosaccharides present in breastmilk with high identification level thanks to ion mobility spectrometry. Four pairs of standard HMO isomers, that are (LNT/LNnT), (LNFP I/LNFP V), (3'-SL/6'-SL) and (2'-FL/3-FL), were first investigated under both positive and negative ionization mode using direct injection-trapped ion mobility spectrometry-time-of-flight mass spectrometry (TIMS-TOF). By examining all the ionic species formed (i.e. protonated and deprotonated ions as well as adduct species), every isomer pair could be distinguished through the separation of at least one species, even with a small difference in collision cross section values (as small as 1.5%) thanks to the flexible resolution capacity of the TIMS instrument. Although multiple mobility peaks resulting from different glycan anomeric conformers, open-ring and/or different ionic isomer structures (i.e. various charge site locations), could be observed for some HMO species. The reduction at the reducing-end of HMOs did not significantly facilitate the isomer distinction. Finally, the unambiguous identification of the studied HMOs in a breastmilk sample showed the potential of the approach combining ion mobility separation and MS/MS experiments for high throughput distinction of HMO isomers in complex breastmilk samples without laborious sample preparation.

Keywords: human milk oligosaccharides, ion mobility-mass spectrometry, isomer, breastmilk

Electronic artwork

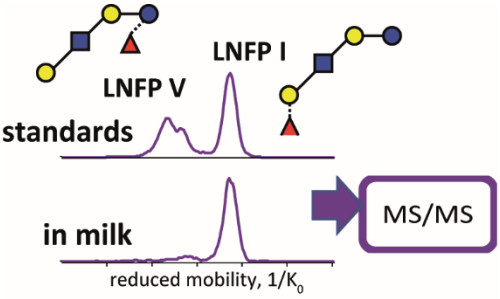

1. Introduction

Breastmilk is the primary source of nutrition for neonates and its biochemical characterization is therefore of great interest. Human milk oligosaccharides (HMOs) are the third most abundant component in breastmilk after lactose and lipids and their concentration ranges from 23 to 5 g/L in colostrum (first milk produced after birth) and mature breastmilk, respectively.[1–3] HMOs are indigestible by the gut of developing infants and instead target bacteria in the neonate large intestine and colon. Thus, HMOs greatly influence the microbiome composition and functions.[1,4] They also appear to protect breastfed infants against microbial infections, acting as a decoy receptor, and to help the development of their immune system.[3,4] All these functions show the need for in-depth HMO analysis.[5] Nevertheless, the oligosaccharide characterization constitutes a great analytical challenge due to the large structural diversity of this compound class. The basic structure of HMOs includes a lactose core at the reducing end, elongated with at least one of five distinct building blocks: D-glucose, D-galactose, N-acetylglucosamine, L-fucose, and N-acetylneuraminic acid (sialic acid) (see **Scheme 1**). Despite a limited number of monosaccharide building blocks, their combination can yield over 100 structures for a single mother and up to 200 HMOs considering breastmilks from multiple mothers.[5,6] This heterogeneity results from the composition (type of monosaccharide building blocks), the connectivity (position of the glycosidic bond, linear or branched sequence) and the configuration (stereochemistry of the glycosidic bond) of the oligosaccharides.

Various analytical tools have been employed for the characterization of oligosaccharides[7,8] and in particular HMOs,[6,9] including Nuclear Magnetic Resonance (NMR) spectroscopy and mass spectrometry (MS). MS is mostly used, especially for complex breastmilk sample analyses thanks to its high sensitivity.[5,7,8] In addition, capillary electrophoresis (CE) has also been widely employed with laser induced fluorescence (LIF)[10] or MS[11] as well as liquid chromatography (LC) hyphenated with MS.[7] Reversed phase (RP), hydrophilic interaction LC (HILIC) and porous graphitic carbon (PGC) are commonly used in LC/MS analyses. Currently, PGC-MS is considered as the most efficient HMO separation platform.[7] Tandem mass spectrometry (MS/MS), in conjunction with (or without) LC, is also essential in structural elucidation, providing the elemental composition determination and connectivity of saccharide residues and in a few cases their configuration.[6,7] Additionally, semi-quantitative or quantitative analyses can be performed through multiple reaction monitoring (MRM) using LC/MS platform as proposed by Mank *et al.*[12] and Csernák *et al*.[13] Currently, more than 200 HMO structures have been characterized from breastmilk samples in term of accurate mass measurements, retention times and fragmentation patterns.[14,15] These hyphenated methods allowed to produce HMO fingerprints and to investigate the relations between infant and maternal characteristics.[16,17] For example, they allowed to classify breastmilks according to the HMOs found.[3,16] HMO profiles mainly depend on the secretor status and Lewis blood group of the mother.[16,18] Secretor mothers yield breastmilk containing α(1,2)-fucose HMOs, while non-secretors do not. This status can drastically affect the substrates available for the microbiota, and thus the composition of the infant gut microbiota. The ratio of secretors/non-secretors varies by ethnicity and geography.[5]

Even if in-depth work has been carried out on glycans and more specifically in HMO analysis, some bottlenecks are still present. First, widely used hyphenated techniques generally require relatively long analysis times (10–60 min) and extensive sample preparation. More importantly, the characterization of HMO structures, especially the resolution of isomers in very complex mixtures, remains challenging.

Ion mobility separation based on the migration of gas phase ions under the effect of a low electric field[19] constitutes an attractive separation technique complementary to conventional LC/MS and CE/MS platforms to characterize complex glycan structures.[20–22] Jin *et al.*[23], for example, demonstrated the ability of ion mobility-mass spectrometry (IM-MS) to resolve the structural complexity of some isomeric glycans, which is not possible by LC/MS alone. Indeed, ion mobility coupled with mass spectrometry has many advantages, the main one being its ability to characterize a large range of positional isomers, conformers but also stereoisomers.[24,25] In addition, IM-MS analyses proceed in a high throughput fashion (a couple of minutes). In some cases, ion mobility separation can be a way to facilitate interpretation of complex samples by revealing the presence of minor compounds from biological matrices.[26] Moreover, ion mobility separation provides a new highly reproducible data feature to ascertain the compound identification: the collision cross section (CCS)[27] and in that respect, efforts have been made to provide CCS databases for the glycan analyses.[28,29] High separation capacity can also be achieved through the incorporation of LC separation into IM-MS instrumentation, allowing a comprehensive three-dimensional (3D) analysis.[30,31] Finally, similar to LC/MS, tandem mass spectrometry can be incorporated into the classical IM-MS platform to produce IM-MS/MS analyses, improving the structural characterization level by the acquisition of CCS and of fragmentation patterns in a single experiment.[20,23,32]

Previous works demonstrated the potential of ion mobility to resolve isomeric oligosaccharides despite their small structural differences. Nevertheless, sophisticated methods are usually required, in which ion mobility separation was combined with chemical covalent derivation,[33] gas phase adduct,[28,34-37] and/or complex ion production[38] as well with prior tandem mass spectrometry experiments.[39,40] Recent technical innovations, such as TIMS,[32,41] Structures for Lossless Ion Manipulations (SLIM),[42] or cyclic Travelling Wave Ion Mobility Spectrometer (cTWIMS),[43,44] have strongly improved the carbohydrate characterization, by increasing the ion mobility separation capacity.

In the present study, high throughput characterization of HMOs was investigated using high resolution trapped ion mobility spectrometry-time of flight mass spectrometry (TIMS-TOF). Few IM-MS studies focused on HMOs have been performed,[28,32,34,36,42] and rarely with the objective of their direct characterization in a complex matrix. We can only cite the work of Struwe et al.[45] who studied two sets of HMO isomers isolated from milk to evaluate the impact of charge location using IM-MS experiments and *ab initio* molecular dynamics. Here, the separation of the HMO isomers was examined in both negative and positive ionization modes. Four isomer pairs of HMOs commonly found in breastmilk samples were studied: i) lacto-N-tetraose (**LNT**) and lacto-N-neotetraose (**LNnT**) (connectivity isomers: β1,3 versus β1,4 linkage), ii) lacto-N-fucopentaose I and V (**LNFP I** and **LNFP V**) (positional isomers: different fucose positions), iii) 2'-fucosyllactose (**2'FL**) and 3-fucosyllactose (**3FL**) (positional isomers: different fucose positions), iv) 3'-sialyllactose (**3'SL**) and 6'-sialyllactose (**6'SL**) (connectivity isomers : α2,3 versus α2,6 linkage). Despite the presence of multiple mobility features for some HMO species, which makes difficult the identification of these isomers, all isomer pairs could be distinguished by considering well-separated HMO species in a global fingerprint. Additionally, the effects of reduction at the reducing end were examined. An overall loss of sensitivity was observed under such conditions while no major improvement in the ion mobility separation or decrease in the number of mobility peaks could be obtained. Finally, the application of IM-MS eventually with MS/MS studies for the direct characterization of HMO isomers in complex

matrices was evaluated. To the best of our knowledge, our work constitutes the first study reporting the direct IM-MS analysis of native HMOs in a breastmilk sample.

2. Experimental Section

2.1. Chemicals and samples

A Select HP water purification system (Purite France eau, Lormont, France) was used to produce ultrapure water with resistivity of 18.2 MΩ.cm. Acetonitrile (ACN, UHPLC grade) was purchased from VWR Chemicals (Fontenay sous Bois, France). Lithium chloride (LiCl), glacial acetic acid, formic acid and sodium borohydride ($NaBH_4$) were obtained from Sigma-Aldrich (Saint Quentin Fallavier, France).

ESI-L low concentration tuning mix, a calibration solution (G1969-85000) was purchased from Agilent Technologies (Santa Clara, CA, USA). Lacto-N-tetraose (LNT), lacto-N-neotetraose (LNnT), lacto-N-fucopentaose I and V (LNFP I and LNFP V), 3'-sialyllactose (3'-SL), 6'-sialyllactose (6'-SL), 2'-fucosyllactose (2'-FL) and 3-fucosyllactose (3-FL) were acquired from Elicityl (Crolles, France) (see structures in **Scheme 1**).

Oligosaccharide standards were studied at a concentration of 0.1 $ng.\mu L^{-1}$ or 1 $ng.\mu L^{-1}$ in ACN/H_2O 50:50 (v/v) in negative ionization and in ACN/H_2O 50:50 (v/v) + 0.1 % formic acid or ACN/H_2O 50:50 (v/v) in positive ionization mode. Lithium chloride (LiCl) was added to enhance cationization (final LiCl concentration of 1 $ng.\mu L^{-1}$) under positive ionization.

Please insert Scheme 1 near here

The mature breastmilk sample was collected from a healthy donor twelve weeks after parturition[47] and stored at -80 °C until analysis. Then 450 µL of water was added to 50 µL of breastmilk. The resulting mixture was centrifuged for 30 min at 3000x*g* to separate lipids. The lower-phase was collected and centrifuged again for 30 min.[48] The obtained lower-phase was then diluted 500 times, corresponding to a final 1:5000 dilution of breastmilk in the appropriate solvent for IM-MS analysis.

2.2. Oligosaccharide reduction[48]

10 µL of HMO standard at 1 µg/µL was diluted by adding 90 µL of water. The resulting sample was then mixed with 100 µL of $NaBH_4$ solution (1 M in 0.1 M NaOH) and incubated for 1 h at 37 °C. The solution was then neutralized by addition of 3 x 4 µL of glacial acetic acid and purified on a Pierce™ graphite spin column (10 mg; Thermo Scientific, les Ulis, France). The reduced standards were eluted 3 times using the same 100 µL of H_2O/ACN (50:50, v/v) solution, and 1 time with an additional 100 µL of H_2O/ACN (50:50, v/v), thus leading to a final volume of 200 µL. Each reduced standard was further diluted for optimal MS analysis.

2.3. Ion mobility spectrometry - mass spectrometry

All IM-MS experiments were conducted on a trapped ion mobility spectrometer – quadrupole – time of flight (Bruker Daltonics, Bremen, Germany) using electrospray ionization (ESI) and direct infusion at a flow rate of 3 $\mu L.min^{-1}$. All operating parameters from the ESI source to the ion mobility cell and mass spectrometer detection were optimized to ensure an optimal response of the studied HMO isomers. Nitrogen was used as both spray and drift gas. The dry gas, capillary temperature and nebulizer gas of the ion source were set at 3.0 $L.min^{-1}$, 250 °C and 0.3 bar, respectively. The end plate offset was maintained at 500 V and the electrospray voltage at – 4500 V and + 3500 V in positive and negative ionization, respectively. For the TIMS analyzer, the Funnel 1 RF, Funnel 2 RF and deflection delta were fixed at 250 Vpp, 250 Vpp and +/- 80 V, respectively. To avoid TIMS saturation, the ion

charge control (ICC) was maintained at 2.0 Mio. The experiments were acquired in the 100 - 1350 *m/z* range using variable mobility ranges (see below) with a transfer time of 70 µs and a pre pulse storage of 5 µs. All parameters were controlled through the oTof control software (Bruker Daltonics).

$^{TIMS}CCS_{N2}$ values were determined from the reduced mobilities, K_0, measured, through a calibration step. Thus, an external calibration for m/z values (in quadratic mode) and reduced mobilities (in linear mode) was carried out before each experiment series using the ESI-L low concentration tuning mix solution. The calibrant ions are detected in positive ionization at *m/z* 322.0481 ($C_6H_{19}N_3O_6P_3^+$), *m/z* 622.0289 ($C_{12}H_{19}F_{12}N_3O_6P_3^+$), *m/z* 922.0098 ($C_{18}H_{19}F_{24}N_3O_6P_3^+$) and *m/z* 1221.9906 ($C_{24}H_{19}F_{36}N_3O_6P_3^+$) with $1/K_0$ values of 0.736, 0.991, 1.199 and 1.393 V.s.cm^{-2}, respectively. For the negative ionization, the calibrant ions are observed at *m/z* 301.9981 ($C_6H_1F_9N_3O_1^-$), *m/z* 601.9790 ($C_{12}H_1F_{21}N_3O_1^-$), *m/z* 1033.9881 ($C_{20}H_{18}F_{27}N_3O_8P_3^-$) and *m/z* 1333.9689 ($C_{26}H_{18}F_{39}N_3O_8P_3^-$) with $1/K_0$ of 0.669, 0.882, 1.258 and 1.407 V.s.cm^{-2}, respectively.

The repeatability and robustness of the ion mobility measurements were assessed. All the experiments were repeated on at least 3 different days and the mean $^{TIMS}CCS_{N2}$ values are reported with a maximum relative standard deviation (RSD) of 0.5 % and an average RSD value of 0.2%, for both ion source polarities. In addition, $^{TIMS}CCS_{N2}$ measurements are not impacted by the compound concentrations. All experiments were conducted for HMO standard concentrations of 0.1 ng.µL^{-1} and 1 ng.µL^{-1} but some HMO analyses were also performed at 0.01 ng.µL^{-1} with no variations in $^{TIMS}CCS_{N2}$ measurements.

The mobility separation resolving power of the TIMS analyzer (see **Equation 1**) can be changed by modifying the scan rate over a defined mobility range.[49] In our study, two types of IM-MS analysis were conducted: i) the first one could be qualified as a "global sample fingerprinting" where inverse reduced mobilities ($1/K_0$) are collected into a range of mobilities of 0.55 – 1.90 V.s.cm^{-2} with a scan rate of 9.52 Hz, providing mobility resolving powers ranging from 50 to 80 (depending on the studied HMO) and ii) the second type refers to a "targeted analysis" focused on a specific m/z value using narrow mobility range detection (typically 0.10 to 0.32 V.s.cm^{-2}) with a scan rate between 2 and 5 Hz and resolving power of 120 to 180. To perform a HMO global fingerprinting (the first IM-MS analysis type), a custom mode was applied and, the mobility range as well as the scan rate were manually optimized to cover the m/z range of 100-1350 (corresponding to CCS range of 100 to 450 Å^2 considering singly-charged ions).

$$R = \frac{K_0}{\Delta K_0} = \frac{CCS}{\Delta CCS} \quad (1)$$

The generated data were manually treated using Data Analysis 5.2 (Bruker Daltonics). All ion mobility spectra reported were extracted from a fixed m/z (mass to charge ratios) of the ionic specie considered. To evaluate the ion mobility separation efficiency, the difference in CCS values, ΔCCS% (see **Equation 2**), was considered as the best criterion for estimating the ion mobility separation capacity. Indeed, the commonly used resolving power was shown to underestimate the real separation capability of some ion mobility instrumentations (e.g., TWIMS).[50]

$$\Delta\mathrm{CCS}\% = \frac{\mathrm{CCS_B} - \mathrm{CCS_A}}{\text{average } \mathrm{CCS_{B,A}}} x\ 100\ (in\ \%) \quad (2)$$

3. Results and Discussion

IM-MS analysis of four HMO isomer pairs (see **Scheme 1**), in native or reduced forms, in a standard mixture or in breastmilk, was conducted using both negative and positive ionization modes to investigate the analytical conditions for an optimal isomer separation (see **experimental section**). In negative ionization mode, deprotonated species, $[M-H]^-$, are mainly produced as well as adduct anions, $[M+Cl]^-$ and $[M+HCOO]^-$. For positive ionization conditions, the mass spectra display more or less abundant protonated molecules, $[M+H]^+$, as well as abundant doubly-charged calcium adducts, $[M+Ca]^{2+}$ and weak sodium adduct peaks, $[M+Na]^+$. The addition of lithium salt was tested to promote the production of adduct ions under positive ESI conditions. Indeed, adduct ions have been reported to enhance mobility separation for various small size isomer compounds[51-53] but also for glycans.[28,34-37] Here, singly-charged $[M+Li]^+$ and doubly charged $[M+2Li]^{2+}$ adducts were detected for some compounds. With the lithium addition, the peak intensities of the $[M+Na]^+$ ions were overall enhanced because the $[M+H]^+$ forms were disfavored resulting in a strong decrease in their intensity.

3.1. IM-MS analysis of native HMOs

The mobility response and separation of all species formed for each native HMO standard were first investigated. A global sample fingerprinting was acquired using large mobility range detection ($1/K_0$ = 0.55-1.90 V.s.cm^{-2}, as global fingerprint) with limited mobility resolving power. More accurate analyses in term of resolution were then conducted by scanning narrow mobility ranges (as targeted analysis, see **experimental section**).

Experimental $^{TIMS}CCS_{N2}$ values obtained from both source polarities are reported in **Tables S1** and **S2**. To investigate more deeply the ability of the TIMS device to resolve HMO isomers, all pairs of isomers were analyzed as binary mixtures (see **Figures S1** and **S2**). The ΔCCS% values obtained from the analyses of all the ionic species of the four isomer pairs are reported in **Table 1** and represented as a heat map according to the experimental ion mobility spectra acquired for the isomer pair mixture. The baseline separation of compounds with ΔCCS% > 3.5% is easily obtained using the large mobility range conditions (i.e. global fingerprint) and the separation of isomers with ΔCCS% > 1.5% is achievable only by using the targeted mode with enhanced resolution.

Please insert Table 1 near here

For the global fingerprint, contrasting results are observed depending on the studied isomer pair and on the ionic species considered (see **Figures S1 and S2**). With resolving powers of about 50-80, baseline separation is only achieved for few species demonstrating the difficulty of characterizing such structurally-closed compounds. **Figure 1** shows the best isomer separation for each HMO pair in positive and negative ESI modes. Overall, the distinction between the **LNT** and **LNnT** isomers is obtained for the $[M+H]^+$, $[M-H]^-$ (see **Figure 1**) and $[M+2Li]^{2+}$ forms (see **Figure S1**), a partial separation is also observed for the $[M+Cl]^-$ adducts (see **Figure S2**). Similarly, the **LNFP I** and **LNFP V** isomers can be well-separated as $[M+H]^+$, $[M-H]^-$ (see **Figure 1**), $[M+2Li]^{2+}$and also $[M+HCOO]^-$ ions , whereas a partial separation is obtained for the $[M+Ca]^{2+}$ and $[M+Cl]^-$ adducts (see **Figures S1** and **S2**). However, both **3'SL/6'SL** and **2'FL/3FL** pairs cannot be separated efficiently, with only partial mobility separation achieved for singly charged lithium adducts (see **Figure 1**).

Please insert Figure 1 near here

Targeted analyses using narrow mobility range detection were also conducted (see **experimental section**). These experiments allowed improving the ion mobility separation with resolving powers of

about 120-180, for all ionic forms of the HMO studied. Mobility responses for all **LNT/LNnT** ionic species with targeted analyses are shown in **Figure 2**. This isomer pair has been particularly investigated because it is not easily separated by conventional liquid chromatography[14,15,48] and constitutes an interesting model of positional isomers.[45] Under high resolution mobility conditions, the **LNT** and **LNnT** isomers are well-separated as $[M+H]^+$, $[M+2Li]^{2+}$, $[M-H]^-$ and $[M-Cl]^-$ species (see **Figure 2**). Good separation is also obtained for $[M+HCOO]^-$ ions whereas only partial separation is observed for the $[M+Li]^+$ ions. However, the sodium adducts could not be separated and the calcium ions did not allow to reach an unambiguous identification (see **Table 1**).

For the **LNFP I/LNFP V** pair, all adduct forms detected could be separated using a targeted analysis and the largest differences in mobility were obtained for the $[M+H]^+$, $[M+2Li]^{2+}$ and $[M-H]^-$ species (see **Table 1**, and their extracted ion mobility spectra in **Figures S1** and **S2**). Importantly, better separation was obtained under high resolution mobility conditions for the **2'FL/3FL** and **3'SL/6'SL** pairs. The distinction of **2'FL/3FL** isomers can be achieved by the baseline mobility separation of the $[M+Li]^+$ and $[M+Cl]^-$ ions as well as by the partial separation for the $[M+Na]^+$ and $[M+HCOO]^-$ adducts (see **Table 1**). In the same fashion, the **3'SL/6'SL** isomers could be separated through the $[M+Li]^+$ and $[M-H]^-$ species (see **Figure 1** and **Table 1**) and a partial separation for $[M+Na]^+$ adducts was observed (see **Figure S1**).

Please insert Figure 2 near here

These results are in accordance with the results already reported,[34,45] *i.e.*, a better mobility separation of the **LNT/LNnT** isomers as $[M-H]^-$ species is observed compared to the sodiated and/or protonated forms. In our study, the ΔCCS% value between the **LNT** and **LNnT** isomers is higher for the $[M-H]^-$ ions (ΔCCS% of 5.8 %) than for the $[M+H]^+$ ions (ΔCCS% of 3.9 % see **Table 1**). Nevertheless, the ΔCCS% values are comparable for the $[M-H]^-$ and $[M+H]^+$ ions of the **LNFP I/LNFP V** couple, with 5.3 % and 5.2 %, respectively (see **Table 1**). No conclusion can be drawn for the **2'FL/3FL** and **3'SL/6'SL** pairs due to the low abundance peak of **3'SL** protonated ions and the absence of signals detected for the protonated **2'FL** and **3FL**. In addition, a good accordance with $^{DTIMS}CCS_{N2}$ values found in the literature[54,55] was obtained with CCS shifts below 1% (see **Table S4**) ; demonstrating that CCS represents a promising compound identification criterion.[56]

No real improvement in mobility separation is obtained by performing metal adduction, in contradiction with previous studies.[28,34-37] The addition of lithium does not allow better ion mobility separation of the corresponding adducts formed. Although the isomer separation can only be achieved with this ionic form for the **2'FL/3FL** and **3'SL/6'SL** pairs (ΔCCS% of 2.6% and 2.5%, respectively, see **Table 1**). The ΔCCS% values are more significant for the $[M+Ca]^{2+}$ species. Nevertheless, the adduct ion formation constitutes an alternative analytical solution, especially for the HMOs which give poor signals for protonated or deprotonated species, for example, from the **2'FL/3FL** isomer pair.

Figures 1 and **2** highlight a critical issue for IM-MS analysis of HMOs. Multiple mobility peaks are often encountered for detected species, especially under high resolution TIMS conditions. A similar phenomenon has been described by other groups also using high resolution instrumentations.[41-43] Ujma *et al.*[43] assigned these multiple peaks to two major anomeric forms (α and β forms) and a minor open-ring form using a heavy oxygen labelling strategy with a cyclic TWIMS in ion mobility/ion mobility mode. Most of the adduct ions formed in positive ESI mode were detected as multiple peaks for at least one isomer (see **Figure S1** or the example of **LNT/LNnT** species in **Figure 2**). Such

observations, already reported,[41-43] could be explained by a variable metal coordination within various glycan conformations, resulting in mobility differences between the different forms. These different forms and conformations can be solved thanks to high resolution TIMS instrument, resulting in the detection of multiple peaks. However, their presence complicates the HMO isomer characterization and, in some cases, prevents unambiguous isomer distinction (independently on the use of large or narrow mobility ranges).

The deprotonated ions of **2'FL/3FL** are, for example, characterized by at least three features (or CCS values) using the large mobility range while the application of targeted mode resulted in the detection of even more peaks (see **Table S2**). In this latter case, the isomer identification cannot be reached due to the presence of several mobility peaks, some of them being overlapped. Otherwise, most of the deprotonated ions from the **LNT/LNnT** and **LNFP I/LNFP V** sets are characterized by two mobility peaks with a major and a minor one (see **Table S2** and **Figure 1**). The minor peak of **LNnT** displays a mobility very close to that of the peak of **LNT** and, similarly the minor peak of **LNFP V** cannot be resolved from the major peak of **LNFP I**, this could be due to low standard compound purity. Nevertheless, for these two isomer pairs, the major peaks are well resolved and characteristics of each HMO structure. Hence, the isomer distinction can be performed under the condition of a comparable MS response, which is less straightforward in complex mixtures. Note that another difficulty in such a direct methodology arises from the varying MS response between isomer ions. The peaks of the protonated ions of **3'SL/6'SL** are, for example, well separated using a global fingerprint mode but **3'SL** gives a much lower response compared to **6'SL** under equimolar conditions and no isomer distinction can be obtained from the mixture of the two compounds (see **Figure S1**). Nevertheless, the direct HMO characterization can be globally performed despite the presence of multiple peaks. For example, the $[M+Li]^+$ forms of both **LNT** and **LNnT** show multiple peaks in the targeted analysis (see **Figure 2D**) but each isomer displays two major specific peaks resolved (ΔCCS% of about 3% between both isomers in **Table 1**). Another example is the distinction of deprotonated **3'SL** and **6'SL** ions, which are detected as two peaks using narrow mobility range (see **Figure 1**). Despite the overlap of a peak of each isomer, the characterization of each isomer is still possible thanks to the detection of a specific mobility peak (ΔCCS% of 2.1% between both isomers; see **Table 1**).

The resolving power and the mobility peak width are also interesting parameters that can be useful in predicting the occurrence of multiple peaks, in particular for less resolving ion mobility instruments. Indeed, a low resolution peak (typically $R_p < 50$) with a FWHM (Full Width at Half Maximum) greater than 0.015 detected in global fingerprinting mode often leads to the multiple peak detection in the targeted analysis. For example, the peaks of the deprotonated forms of 3'SL and 6'SL show signals with resolving powers of 50 and 48, respectively and FWHM of 0.023 and 0.024, respectively in the global fingerprinting mode while two resolved peaks appeared for each deprotonated isomer in the targeted analysis (see **Figures 1** and **S2**).

Hence, the presence of multiple and/or unresolved peaks can make difficult the HMO identification and no general trend can be obtained for all the HMOs. Nevertheless, all species detected both in positive and negative ion modes can be distinguished when analyzing complex mixtures as the data of all detected species can altogether allow conclusions to be drawn about the isomer pair studied (see **section 3.3**).

3.2. IM-MS analysis of reduced HMOs

The detection of multiple signals for native HMO species has been explained by the existence of different conformations (see the discussion upper and the work of Ujma *et al.*[43]). Typically, the glycan reduction is commonly performed prior to the LC separation to avoid the chromatogram artefactual complexification resulting from the chromatographic separation of alpha/beta anomers (i.e. peak splitting).[57] In our study, all isomer couples were reduced and analyzed by IM-MS analyses in both

negative and positive polarities. However, reduced HMOs showed weak MS sensitivity under negative ion mode and no ion mobility experiments could be conducted. For the positive ionization mode, better MS responses could be obtained and only the global sample fingerprints are acquired for the reduced forms (see **Table S3** and **Figure S3**). A comparison of isomer separation between native and reduced forms is reported in **Figure 3**, for some ionic species of HMO pairs detected under positive ESI conditions (all IM-MS analyses from reduced HMOs can be found in **Figure S3**).

Please insert Figure 3 near here

Contrasting results were obtained according to the isomer pair and the ionic species studied. Overall, no real improvement in mobility separation was achieved after reduction. **Figure 3** shows poorer separations for the $[M+Ca]^{2+}$ species of reduced **LNFP I/LNFP V** and for the $[M+Li]^{+}$ ions of reduced **3'SL/6'SL** compared to their native forms, while a small separation improvement is obtained for the $[M+Na]^{+}$ adducts of the reduced **2'FL/3FL** pair. Nevertheless, the protonated $[M+H]^{+}$ ions of the reduced **LNT/LNnT** and **LNFP I/LNFP V** forms are better separated than the $[M+H]^{+}$ ions of their native forms (see **Figures 3** and **S3**).

It should be noted that, despite the decrease in their number, multiple peaks are still observed from reduced HMOs. For example, multiple peaks are detected for the protonated ions of the reduced **LNT/LNnT** and **LNFP I/LNFP V** forms (see **Figure 2** and **S3**, respectively). Wei *et al.*[32] recently reported a similar observation with permethylated isomeric glycans, with the reducing-end reduction not decreasing the number of mobility peaks detected. Hence, the multiple mobility features could result from multiple ion structures, i.e. with various charge locations for a given species.[42,58]

These results enlightened the difficulty to characterize the high heterogeneity of glycans. In addition to the glycan structural variety, the existence of anomeric configurations (α and β) and to a lesser extent of large ion populations makes very difficult the prediction of a general trend for all HMOs. Nevertheless, these preliminary studies on HMO standards provide a very promising analytical solution to characterize HMOs in breastmilk using IM-MS.

3.3. Direct IM-MS and IM-MS/MS analysis of breastmilk

Direct and fast IM-MS analysis of a breastmilk sample was then performed without extensive sample preparation (only a defatted protocol was applied, see **experimental section**). IM-MS experiments were conducted on a breastmilk sample diluted 1:5000 under both positive (see **Figure S4**) and negative (see **Figure 4**) ionization modes. Large mobility range detection was first applied to acquire a global HMO profile. Nevertheless, a targeted method using a narrow mobility range is then applied to screen for specific ionic forms (see the extracted ion mobility spectrum of deprotonated **3'SL** and **6'SL** ions detected in milk using a targeted analysis in **Figure 4**). **Figure 4** shows the IM-MS analysis under negative ESI mode of a diluted breastmilk sample. The extracted ion mobility spectra of the $[M-H]^{-}$, $[M+Cl]^{-}$ and $[M+HCOO]^{-}$ ions for the four native HMOs isomer pairs were reported from both standard mixture solution (final concentration at 1 $ng.\mu L^{-1}$) and diluted breastmilk sample.

As described in the previous section, isomer separation cannot be achieved for all HMO ionic species. Nevertheless, by combining the results from all the different ions, the distinction of most of the isomers can be successfully obtained under global fingerprinting conditions (see **Figure 4**). Indeed, **LNFP I** and **LNFP V** are well or partially separated for all the ionic forms considered. The $[M+HCOO]^-$ ions of **LNT** and **LNnT** are not detected in the diluted breastmilk sample but these two isomers can be distinguished by the $[M-H]^-$ and $[M+Cl]^-$ ions. The characterization of the **2'FL/3FL** pair is more complicated since these two isomers are not separated as $[M-H]^-$ ions (see **Figure S2** and **Figure 4**) but a partial separation is obtained for the $[M+Cl]^-$ adducts and the mobility peak width of the $[M+HCOO]^-$ ions suggests the presence of the two isomers under the same mobility peak. Finally, **3'SL/6'SL** is the sole isomer pair that cannot be resolved using a large mobility range because the only $[M-H]^-$ ions detected display a single broad peak under moderate resolution conditions. Nevertheless, the targeted analysis on these deprotonated ions showed the presence of the two isomers (detected as multiple ion mobility peaks), which are successfully distinguished (see comparison of **Figure 1** and **Figure 4**).

Similar observations can be made from IM-MS analysis under positive ion conditions (see the acquired global fingerprint in **Figure S4**), where the **LNT/LNnT** and **LNFP I/LNFP V** pairs are distinguished from the extracted ion mobility spectra of $[M+H]^+$ ions while the peak width of the $[M+Na]^+$ form for **2'FL/3FL** allow to figure out the presence of both isomers. The **3'SL/6'SL** pair is still the most difficult to be distinguished in global fingerprinting mode but the detection of the $[M+Ca]^{2+}$ species gives an insight on the presence of one of the isomers or the other (see **Table 1** and **Figure S1**). Finally, an accurate isomer characterization can be obtained by combining all data from both positive and negative ion modes (**Figures 4** and **S4**).

IM-MS analysis of HMO standard mixture reveals another striking observation that is the variable MS response among HMO structures. A much higher intensity of mobility signal is, for example, observed for the $[M-H]^-$ ions of **3'SL/6'SL** isomers compared to other deprotonated HMO ions (see **Figure 4**).

Please insert Figure 4 near here

Interestingly, the comparison of HMO responses under IM-MS analysis between the standard mixture under equimolar conditions and the breastmilk sample suggested a much lower amount of **LNFP V** and **3FL** relatively to their respective isomers in the breastmilk sample. Indeed, the mobility peaks of all the ionic forms of the **LNFP V** compound are clearly absent in the breastmilk sample under both negative (**Figure 4**) and positive (**Figure S4**) ion modes. A much lower relative amount of **3FL** compared to **2'FL** can also be evidenced by the disappearance of the peak shoulder for the $[M+Cl]^-$ and $[M+Na]^+$ ions which corroborates a smaller width of the unresolved peak of $[M+HCOO]^-$ ions in the breastmilk sample (see **Figures 4** and **S4)**. In fact, a lower relative amount of these two HMOs (**LNFP V** and **3FL**) compared to their respective isomers has already been reported by previous LC/MS experiments.[48] To check that the absence of their mobility peaks is not caused by matrix effects, IM-MS analysis of a diluted breastmilk sample spiked with the corresponding authentic standard at 1 $ng.\mu L^{-1}$ was performed under the same conditions (see **Figure S5**). The detection of mobility signals corresponding to the two spiked **LNFP V** and **3FL** indicated that these compounds could be detected in breastmilk, but their response is lower in such a matrix compared to their analogous standard compounds in a solvent solution. Such an encouraging result shows the possibility of performing a relative quantification of one isomer to another using the direct IM-MS approach. Of course, further investigations are needed to develop and validate a semi-quantitative method in terms of detection limit, response linearity, reproducibility, and matrix effects for accurate

quantification of HMOs. Few works have reported a tentative estimation of the relative content of (isomeric) compounds[25,41] using IM-MS approach, with, for example, a detection limit of 0.1% between sugar anomers.[25]

To further investigate the breastmilk sample, the search for other HMOs was performed based on their theoretical accurate m/z values and their corresponding extracted mobility spectra were reported (see **Table S5 and S6**). Although the monosaccharide composition can be unambiguously assigned thanks to the accurate mass measurements, the experimental $^{TIMS}CCS_{N2}$ values cannot be attributed to a specific HMO structure without authentic standard compounds. Indeed, our results demonstrated the possibility for a given HMO structure to display multiple ion mobility peaks due to different HMO configurations and/or ion isomers. The availability of pure standards is therefore mandatory in order to unambiguously build a reference HMO mobility database.

Finally, in addition to IM-MS analysis, tandem mass spectrometry (MS/MS) experiments were performed on the breastmilk sample, providing three data features for a high degree of compound identification (m/z, fragmentation pattern and $^{TIMS}CCS_{N2}$) in a single experiment (see **Figure 4**). With our ion source parameters, no in-source fragmentation is detected under ESI conditions. Therefore, collision-induced dissociation (CID) experiments were systematically performed on both protonated and deprotonated precursor ions after their ion mobility separations. The CID spectra display in both positive and negative modes mostly cleavages of glycosidic bond, yielding B, Y or C, Z type ions with little or no cross-ring fragment ions (A and X ions) according to the Domon and Costello nomenclature.[59] It must be noted that glycan rearrangements (typically fucose residue) may occur in MS/MS experiments for protonated species using CID conditions.[60]

The obtained data were compared to the MS/MS experiments carried out for the HMO standards. **Figures 4, S4** and **S6** show the MS/MS spectra of some HMOs which can be distinguished by ion mobility and which exhibit distinct spectral fingerprints and/or isomer diagnostic ions. Note that a better isomer distinction based on specific isomer fragment ions was obtained from the deprotonated LNFP I/LNFPV pair, compared to positive ion conditions, as already reported by Mank et al.[12] It should be emphasized that although the $[M-H]^-$ ions of **3'SL** and **6'SL** are not separated using the global fingerprinting mode, the specific fragmentation patterns of each isomer can be obtained by performing a targeted analysis (see MS/MS spectra obtained from the mobility peaks A and C detected under targeted conditions in **Figure 4**). Nevertheless, it is still possible to extract an isomer-specific fragmentation pattern from an unresolved ion mobility peak detected in large mobility mode by extracting the MS/MS spectra at the edges of the peak (see **Figure S6**).

4. Conclusion

Breastmilk characterization is challenging due to the diversity of HMOs and their structural complexity. This study shows the potential of direct injection TIMS-TOF for high throughput and high resolution analyses of the most abundant HMOs without extensive sample preparation of breastmilk. The IM-MS analyses allowed to identify all the HMO pairs studied by combining the different species detected in both ion polarities (positive and negative ESI modes). With such a direct IM-MS analysis, some semi-quantitative hypotheses could even be made about the breastmilk components. In addition, the flexible resolution of TIMS enabled to perform both global fingerprints and targeted analyses on the same sample. Finally, MS/MS experiments after mobility separation of the isomer species allowed to increase the level of confidence in the compound identification, by providing

three molecular descriptors obtained in a single analysis (CCS, m/z and fragmentation patterns). Our results constitute the proof of concept study of the application of the direct IM-MS approach as a high throughput analytical platform for the characterization of HMOs in breastmilk. It could, for example, be used for the classification of secretor status without lengthy LC-MS analyses. Further investigations on other HMO standards are required to build an HMO database that includes ion mobility and fragmentation pattern data useful for identifying as many HMOs as possible in breastmilk.

ACKNOWLEDGMENTS

We thank the MetaboHUB infrastructure (ANR-11-INBS-0010 grant) for the funding.

References

(1) Zivkovic, A. M.; German, J. B.; Lebrilla, C. B.; Mills, D. A. Human Milk Glycobiome and Its Impact on the Infant Gastrointestinal Microbiota. *Proc. Natl. Acad. Sci.* **2011**, *108* (Supplement_1), 4653–4658. https://doi.org/10.1073/pnas.1000083107.

(2) Mehra, R.; Kelly, P. Milk Oligosaccharides: Structural and Technological Aspects. *Int. Dairy J.* **2006**, 7. https://doi.org/10.1016/j.idairyj.2006.06.008.

(3) Plaza-Díaz, J.; Fontana, L.; Gil, A. Human Milk Oligosaccharides and Immune System Development. *Nutrients* **2018**, *10* (8), 1038. https://doi.org/10.3390/nu10081038.

(4) Quin, C.; Vicaretti, S. D.; Mohtarudin, N. A.; Garner, A. M.; Vollman, D. M.; Gibson, D. L.; Zandberg, W. F. Influence of Sulfonated and Diet-Derived Human Milk Oligosaccharides on the Infant Microbiome and Immune Markers. *J. Biol. Chem.* **2020**, *295* (12), 4035–4048. https://doi.org/10.1074/jbc.RA119.011351.

(5) Amicucci, M. J.; Nandita, E.; Lebrilla, C. B. Function without Structures: The Need for In-Depth Analysis of Dietary Carbohydrates. *J. Agric. Food Chem.* **2019**, *67* (16), 4418–4424. https://doi.org/10.1021/acs.jafc.9b00720.

(6) Porfirio, S.; Archer-Hartmann, S.; Moreau, G. B.; Ramakrishnan, G.; Haque, R.; Kirkpatrick, B. D.; Petri, W. A.; Azadi, P. New Strategies for Profiling and Characterization of Human Milk Oligosaccharides. *Glycobiology* **2020**, *30* (10), 774–786. https://doi.org/10.1093/glycob/cwaa028.

(7) Kailemia, M. J.; Ruhaak, L. R.; Lebrilla, C. B.; Amster, I. J. Oligosaccharide Analysis by Mass Spectrometry: A Review of Recent Developments. *Anal. Chem.* **2014**, *86* (1), 196–212. https://doi.org/10.1021/ac403969n.

(8) Mirgorodskaya, E.; Karlsson, N. G.; Sihlbom, C.; Larson, G.; Nilsson, C. L. Cracking the Sugar Code by Mass Spectrometry: An Invited Perspective in Honor of Dr. Catherine E. Costello, Recipient of the 2017 ASMS Distinguished Contribution Award. *J. Am. Soc. Mass Spectrom.* **2018**, *29* (6), 1065–1074. https://doi.org/10.1007/s13361-018-1912-3.

(9) Ruhaak, L. R.; Lebrilla, C. B. Advances in Analysis of Human Milk Oligosaccharides. *Adv. Nutr.* **2012**, *3* (3), 406S-414S. https://doi.org/10.3945/an.112.001883.

(10) Mantovani, V.; Galeotti, F.; Maccari, F.; Volpi, N. Recent Advances in Capillary Electrophoresis Separation of Monosaccharides, Oligosaccharides, and Polysaccharides. *ELECTROPHORESIS* **2018**, *39* (1), 179–189. https://doi.org/10.1002/elps.201700290.

(11) Mechref, Y.; Novotny, M. V. Glycomic Analysis by Capillary Electrophoresis–Mass Spectrometry. *Mass Spectrom. Rev.* **2009**, *28* (2), 207–222. https://doi.org/10.1002/mas.20196.

(12) Mank, M.; Welsch, P.; Heck, A. J. R.; Stahl, B. Label-Free Targeted LC-ESI-MS2 Analysis of Human Milk Oligosaccharides (HMOS) and Related Human Milk Groups with Enhanced Structural Selectivity. *Anal Bional Chem* **2018**, *411*, 231-250. https://doi.org/10.1007/s00216-018-1434-7.

(13) Csernák, O.; Rácz, B.; Alberti, Á.; Béni, S. Quantitative Analysis of 3'- and 6'-Sialyllactose in Human Milk Samples by HPLC-MS/MS: A Validated Method for the Comparison of Two Consecutive Lactation Periods in the Same Woman. *J. Pharm. Biomed. Anal.* **2020**, *184*, 113184. https://doi.org/10.1016/j.jpba.2020.113184.

(14) Wu, S.; Tao, N.; German, J. B.; Grimm, R.; Lebrilla, C. B. Development of an Annotated Library of Neutral Human Milk Oligosaccharides. *J. Proteome Res.* **2010**, *9* (8), 4138–4151. https://doi.org/10.1021/pr100362f.

(15) Remoroza, C. A.; Mak, T. D.; De Leoz, M. L. A.; Mirokhin, Y. A.; Stein, S. E. Creating a Mass Spectral Reference Library for Oligosaccharides in Human Milk. *Anal Chem* **2018**, 12. https://doi.org/10.1021/acs.analchem.8b01176.

(16) Wang, M.; Zhao, Z.; Zhao, A.; Zhang, J.; Wu, W.; Ren, Z.; Wang, P.; Zhang, Y. Neutral Human Milk Oligosaccharides Are Associated with Multiple Fixed and Modifiable Maternal and Infant Characteristics. *Nutrients* **2020**, *12* (3), 826. https://doi.org/10.3390/nu12030826.

(17) Azad, M. B.; Robertson, B.; Atakora, F.; Becker, A. B.; Subbarao, P.; Moraes, T. J.; Mandhane, P. J.; Turvey, S. E.; Lefebvre, D. L.; Sears, M. R.; Bode, L. Human Milk Oligosaccharide Concentrations Are Associated with Multiple Fixed and Modifiable Maternal Characteristics, Environmental Factors, and Feeding Practices. *J Nutr* **2018**, *148* (11), 1733-1742. https://doi.org/10.1093/jn/nxy175.

(18) Kunz, C.; Meyer, C.; Collado, M. C.; Geiger, L.; García-Mantrana, I.; Bertua-Ríos, B.; Martínez-Costa, C.; Borsch, C.; Rudloff, S. Influence of Gestational Age, Secretor, and Lewis Blood Group Status on the Oligosaccharide Content of Human Milk. *J. Pediatr. Gastroenterol. Nutr.* **2017**, *64* (5), 789–798. https://doi.org/10.1097/MPG.0000000000001402.

(19) Dodds, J. N.; Baker, E. S. Ion Mobility Spectrometry: Fundamental Concepts, Instrumentation, Applications, and the Road Ahead. *J. Am. Soc. Mass Spectrom.* **2019**, *30* (11), 2185–2195. https://doi.org/10.1007/s13361-019-02288-2.

(20) Hofmann, J.; Pagel, K. Glycan Analysis by Ion Mobility–Mass Spectrometry. *Angew Chem Int Ed* **2017**, *56* (8),8342-8349. https://doi.org/10.1002/anie.201701309.

(21) Morrison, K. A.; Clowers, B. H. Contemporary Glycomic Approaches Using Ion Mobility–Mass Spectrometry. *Curr. Opin. Chem. Biol.* **2018**, *42*, 119–129. https://doi.org/10.1016/j.cbpa.2017.11.020.

(22) Mu, Y.; Schulz, B.; Ferro, V. Applications of Ion Mobility-Mass Spectrometry in Carbohydrate Chemistry and Glycobiology. *Molecules* **2018**, *23* (10), 2557. https://doi.org/10.3390/molecules23102557.

(23) Jin, C.; Harvey, D. J.; Struwe, W. B.; Karlsson, N. G. Separation of Isomeric O-Glycans by Ion Mobility and Liquid Chromatography–Mass Spectrometry. *Anal Chem* **2019**, *91* (16), 10604-10613 https://doi.org/10.1021/acs.analchem.9b01772.

(24) Wu, Q.; Wang, J.-Y.; Han, D.-Q.; Yao, Z.-P. Recent Advances in Differentiation of Isomers by Ion Mobility Mass Spectrometry. *TrAC Trends Anal. Chem.* **2020**, *124*, 115801. https://doi.org/10.1016/j.trac.2019.115801.

(25) Hofmann, J.; Hahm, H. S.; Seeberger, P. H.; Pagel, K. Identification of Carbohydrate Anomers Using Ion Mobility–Mass Spectrometry. *Nature* **2015**, *526* (7572), 241–244. https://doi.org/10.1038/nature15388.

(26) Harvey, D. J.; Sobott, F.; Crispin, M.; Wrobel, A.; Bonomelli, C.; Vasiljevic, S.; Scanlan, C. N.; Scarff, C. A.; Thalassinos, K.; Scrivens, J. H. Ion Mobility Mass Spectrometry for Extracting Spectra of N-Glycans Directly from Incubation Mixtures Following Glycan Release: Application to Glycans from Engineered Glycoforms of Intact, Folded HIV Gp120. *J. Am. Soc. Mass Spectrom.* **2011**, *22* (3), 568–581. https://doi.org/10.1007/s13361-010-0053-0.

(27) May, J. C.; Morris, C. B.; McLean, J. A. An Ion Mobility Collision Cross Section Compendium. *Anal Chem* **2017**, 27. https://doi.org/10.1021/acs.analchem.6b04905.

(28) Fenn, L. S.; McLean, J. A. Structural Resolution of Carbohydrate Positional and Structural Isomers Based on Gas-Phase Ion Mobility-Mass Spectrometry. *Phys Chem Chem Phys* **2011**, *13* (6), 2196–2205. https://doi.org/10.1039/C0CP01414A.

(29) Struwe, W. B.; Pagel, K.; Benesch, J. L. P.; Harvey, D. J.; Campbell M. P. GlocoMob: an ion mobility-mass spectrometry collision cross section database for glycomics. *Glycoconj J* 2016, 33, 399-404. https://doi.org/10.1007/s10719-015-9613-7

(30) Lareau, N. M.; May, J. C.; McLean, J. A. Non-Derivatized Glycan Analysis by Reverse Phase Liquid Chromatography and Ion Mobility-Mass Spectrometry. *The Analyst* **2015**, *140* (10), 3335–3338. https://doi.org/10.1039/C5AN00152H.

(31) Yamaguchi, Y.; Nishima, W.; Re, S.; Sugita, Y. Confident Identification of Isomeric *N* -Glycan Structures by Combined Ion Mobility Mass Spectrometry and Hydrophilic Interaction Liquid Chromatography: Identification of Isomeric *N* -Glycans by IM-MS and HILIC. *Rapid Commun. Mass Spectrom.* **2012**, *26* (24), 2877–2884. https://doi.org/10.1002/rcm.6412.

(32) Wei, J.; Tang, Y.; Ridgeway, M. E.; Park, M. A.; Costello, C. E.; Lin, C. Accurate Identification of Isomeric Glycans by Trapped Ion Mobility Spectrometry-Electronic Excitation Dissociation Tandem Mass Spectrometry. *Anal. Chem.* **2020**, *92* (19), 13211–13220. https://doi.org/10.1021/acs.analchem.0c02374.

(33) Li, L.; McKenna, K. R.; Li, Z.; Yadav, M.; Krishnamurthy, R.; Liotta, C. L.; Fernández, F. M. Rapid resolution of carbohydrate isomers via multi-site derivatization ion mobility-mass spectrometry. *The Analyst* **2018**, 143, 949-955. https://doi.org/10.1039/C7AN01796K.

(34) Zheng, X.; Zhang, X.; Schocker, N. S.; Renslow, R. S.; Orton, D. J.; Khamsi, J.; Ashmus, R. A.; Almeida, I. C.; Tang, K.; Costello, C. E.; Smith, R. D.; Michael, K.; Baker, E. S. Enhancing Glycan Isomer Separations with Metal Ions and Positive and Negative Polarity Ion Mobility Spectrometry-Mass Spectrometry Analyses. *Anal. Bioanal. Chem.* **2017**, *409* (2), 467–476. https://doi.org/10.1007/s00216-016-9866-4.

(35) Xie, C.; Wu, Q.; Zhang, S.; Wang, C.; Gao, W.; Yu, J.; Tang, K. Improving Glycan Isomeric Separation via Metal Ion Incorporation for Drift Tube Ion Mobility-Mass Spectrometry. *Talanta* **2020**, *211*, 120719. https://doi.org/10.1016/j.talanta.2020.120719.

(36) Huang, Y.; Dodds, E. D. Ion Mobility Studies of Carbohydrates as Group I Adducts: Isomer Specific Collisional Cross Section Dependence on Metal Ion Radius. *Anal. Chem.* **2013**, *85* (20), 9728–9735. https://doi.org/10.1021/ac402133f.

(37) Huang, Y.; Dodds, E. D. Discrimination of Isomeric Carbohydrates as the Electron Transfer Products of Group II Cation Adducts by Ion Mobility Spectrometry and Tandem Mass Spectrometry. *Anal Chem* **2015**, *87* (11), 5664–5668. https://doi.org/10.1021/acs.analchem.5b00759

(38) Gaye, M. M.; Nagy, G.; Clemmer, D.E.; Pohl, N. L. B. Multidimensional analysis of 16 glucose isomers by ion mobility spectrometry. *Anal Chem* **2016**, 88:2335–2344. https://doi.org/10.1021/acs.analchem.5b04280

(39) Li, H.; Bendiak, B.; Siems, W. F.; Gang, D. R.; Hill, H. H. Ion Mobility Mass Spectrometry Analysis of Isomeric Disaccharide Precursor, Product and Cluster Ions: Analysis of Isomeric Disaccharide Precursor, Product and Cluster Ions. *Rapid Commun. Mass Spectrom.* **2013**, *27* (23), 2699–2709. https://doi.org/10.1002/rcm.6720.

(40) Hofmann, J.; Stuckmann, A.; Crispin, M.; Harvey, D. J.; Pagel, K.; Struwe, W. B. Identification of Lewis and Blood Group Carbohydrate Epitopes by Ion Mobility-Tandem-Mass Spectrometry Fingerprinting. *Anal Chem* **2017**, 89, 2318-2325. https://doi.org/10.1021/acs.analchem.6b03853

(41) Przybylski, C.; Bonnet, V. Discrimination of Isomeric Trisaccharides and Their Relative Quantification in Honeys Using Trapped Ion Mobility Spectrometry. *Food Chem.* **2021**, 341:128182. https://doi.org/10.1016/j.foodchem.2020.128182.

(42) Nagy, G.; Attah, I. K.; Garimella, S. V. B.; Tang, K.; Ibrahim, Y. M.; Baker, E. S.; Smith, R. D. Unraveling the Isomeric Heterogeneity of Glycans: Ion Mobility Separations in Structures for Lossless Ion Manipulations. *Chem. Commun.* **2018**, *54* (83), 11701–11704. https://doi.org/10.1039/C8CC06966B.

(43) Ujma, J.; Ropartz, D.; Giles, K.; Richardson, K.; Langridge, D.; Wildgoose, J.; Green, M.; Pringle, S. Cyclic Ion Mobility Mass Spectrometry Distinguishes Anomers and Open-Ring Forms of Pentasaccharides. *J. Am. Soc. Mass Spectrom.* **2019**, *30* (6), 1028–1037. https://doi.org/10.1007/s13361-019-02168-9.

(44) Ropartz, D.; Fanuel, M.; Ujma, J.; Palmer, M.; Giles, K.; Rogniaux, H. Structure Determination of Large Isomerci Oligosaccharides of Natural Origin through Multipass and Multistage Cyclic Traveling-Wave Ion Mobility Mass Spectrometry. *Anal Chem* **2019**, 91 (18), 12030-12037. https://doi.org/10.1021/acs.analchem.9b03036

(45) Struwe, W. B.; Baldauf, C.; Hofmann, J.; Rudd, P. M.; Pagel, K. Ion Mobility Separation of Deprotonated Oligosaccharide Isomers – Evidence for Gas-Phase Charge Migration. *Chem. Commun.* **2016**, *52* (83), 12353–12356. https://doi.org/10.1039/C6CC06247D.

(46) Neelamegham, S.; Aoki-Kinoshita, K.; Bolton, E.; Frank, M.; Lisacek, F.; Lütteke, T.; O'Boyle, N.; Packer, N. H.; Stanley, P.; Toukach, P.; Varki, A.; Woods, R. J.; The SNFG Discussion Group; Darvill, A.; Dell, A.; Henrissat, B.; Bertozzi, C.; Hart, G.; Narimatsu, H.; Freeze, H.; Yamada, I.; Paulson, J.; Prestegard, J.; Marth, J.; Vliegenthart, J. F. G.; Etzler, M.; Aebi, M.; Kanehisa, M.; Taniguchi, N.; Edwards, N.; Rudd, P.; Seeberger, P.; Mazumder, R.; Ranzinger, R.; Cummings, R.; Schnaar, R.; Perez, S.; Kornfeld, S.; Kinoshita, T.; York, W.; Knirel, Y. Updates to the Symbol Nomenclature for Glycans Guidelines. *Glycobiology* **2019**, *29* (9), 620–624. https://doi.org/10.1093/glycob/cwz045.

(47) Bernard, H.; Ah-Leung, S.; Drumare, M.-F.; Feraudet-Tarisse, C.; Verhasselt, V.; Wal, J.-M.; Créminon, C.; Adel-Patient, K. Peanut Allergens Are Rapidly Transferred in Human Breast Milk and Can Prevent Sensitization in Mice. *Allergy* **2014**, *69* (7), 888–897. https://doi.org/10.1111/all.12411.

(48) Oursel, S.; Cholet, S.; Junot, C.; Fenaille, F. Comparative Analysis of Native and Permethylated Human Milk Oligosaccharides by Liquid Chromatography Coupled to High Resolution Mass Spectrometry. *J. Chromatogr. B* **2017**, *1071*, 49–57. https://doi.org/10.1016/j.jchromb.2017.03.028.

(49) Ridgeway, M. E.; Lubeck, M.; Jordens, J.; Mann, M.; Park, M. A. Trapped Ion Mobility Spectrometry: A Short Review. *Int. J. Mass Spectrom.* **2018**, *425*, 22–35. https://doi.org/10.1016/j.ijms.2018.01.006.

(50) Dodds, J. N.; May, J. C.; McLean, J. A. Correlating Resolving Power, Resolution, and Collision Cross Section: Unifying Cross-Platform Assessment of Separation Efficiency in Ion Mobility Spectrometry. *Anal. Chem.* **2017**, *89* (22), 12176–12184. https://doi.org/10.1021/acs.analchem.7b02827.

(51) Delvaux, A.; Rathahao-Paris, E.; Alves, S. An Emerging Powerful Technique for Distinguishing Isomers: Trapped Ion Mobility Spectrometry Time-of-flight Mass Spectrometry for Rapid Characterization of Estrogen Isomers. *Rapid Commun. Mass Spectrom.* **2020**, *34*, 8928. https://doi.org/10.1002/rcm.8928.

(52) Rister, A. L.; Martin, T. L.; Dodds, E. D. Application of Group I Metal Adduction to the Separation of Steroids by Traveling Wave Ion Mobility Spectrometry. *J Am Soc Mass Spectrom* **2019**, 30(2)248-255. https://doi.org/10.1021/jasms.8b05945.

(53) Zietek, B. M.; Mengerink, Y.; Jordens, J.; Somsen, G. W.; Kool, J.; Honing, M. Adduct-Ion Formation in Trapped Ion Mobility Spectrometry as a Potential Tool for Studying Molecular Structures and Conformations. *Int. J. Ion Mobil. Spectrom.* **2018**, *21* (1–2), 19–32. https://doi.org/10.1007/s12127-017-0227-6.

(54) Zheng, X.; Aly, N. A.; Zhou, Y.; Dupuis, K. T.; Bilbao, A.; Paurus, V. L.; Orton, D. J.; Wilson, R.; Payne, S. H.; Smith, R. D.; Baker, E. S. A Structural Examination and Collision Cross Section Database for over 500 Metabolites and Xenobiotics Using Drift Tube Ion Mobility Spectrometry. *Chem. Sci.* **2017**, 8, 7724-7736. https://doi.org/10.1039/c7sc03464d.

(55) May, J. C.; Goodwin, C. R.; Lareau, N. M.; Leaptrot, K. L.; Morris, C. B.; Kurulugama, R. T.; Mordehai, A.; Klein, C.; Barry, W.; Darland, E.; Overney, G.; Imatani, K.; Sta, G. C. Conformational Ordering of Biomolecules in the Gas Phase: Nitrogen Collision Cross Sections Measured on a Prototype High Resolution Drift Tube Ion Mobility-Mass Spectrometer. *Anal Chem* **2014**, 86, 2107-2116. https://doi.org/10.1021/ac4038448.

(56) Paglia, G.; Astarita, G. Metabolomics and Lipidomics Using Traveling-Wave Ion Mobility Mass Spectrometry. *Nat. Protoc.* **2017**, *12* (4), 797–813. https://doi.org/10.1038/nprot.2017.013.

(57) Ritamo, I.; Räbinä, J.; Natunen, S.; Valmu, L. Nanoscale Reversed-Phase Liquid Chromatography–Mass Spectrometry of Permethylated N-Glycans. *Anal. Bioanal. Chem.* **2013**, *405* (8), 2469–2480. https://doi.org/10.1007/s00216-012-6680-5.

(58) Oranzi, N. R.; Kemperman, R. H. J.; Wei, M. S.; Petkovska, V. I.; Granato, S. W.; Rochon, B.; Kaszycki, J.; La Rotta, A.; Dit Fouque, K. J.; Fernandez-Lima, F.; Yost, R. A. Measuring the Integrity of Gas-Phase Conformers of Sodiated 25-Hydroxyvitamin D3 by Drift Tube, Traveling Wave, Trapped, and High-Field Asymmetric Ion Mobility. *Anal Chem* **2019**, 91, 4092-4099. https://doi.org/10.1021/acs.analchem.8b05723.

(59) Domon, B.; Costello, C. E. A Systematic Nomenclature for Carbohydrate Fragmentations in FAB-MS/MS Spectra of Glycoconjugates. *Glycoconj. J.* **1988**, *5* (4), 397–409. https://doi.org/10.1007/BF01049915.

(60) Wuhrer, M.; Deelder, A. M.; van der Burgt, Y. E. M. Mass Spectrometric Glycan Rearrangements. *Mass Spectrom. Rev.* **2011**, *30* (4), 664–680. https://doi.org/10.1002/mas.20337.

Figures and tables captions:

Table 1: ΔCCS% values of all ionic species detected for the isomer pairs studied. The table shows a heat map, based on the IM-MS separation of each isomer pair mixture and depending on the IM-MS conditions applied: the global fingerprinting (in bold) versus targeted (in bracket) modes.

Scheme 1: Structures of the isomer pairs of HMO studied (according to the Symbol Nomenclature for Graphical Representation of Glycans[46])

Figure 1: Extracted ion mobility spectra of different HMO isomer species, corresponding to the best isomer mobility separation under both positive and negative ESI modes using large mobility range detection, excepted (in D) for the deprotonated ions of 3'SL/6'SL pair for which a targeted mode is applied for their separation. *All HMOs were injected alone (colored plots) or in binary mixtures (dashed plots) at a concentration of 1 ng.µL^{-1}.*

Figure 2: Extracted ion mobility spectra of all LNT and LNnT detected ions under both positive and negative ESI modes, using narrow mobility range detection mode (high resolution conditions). *Each HMO was injected at a concentration of 0.1 ng.µL^{-1}. In D) and E), results were obtained for positive ESI mode after addition of lithium at 1 ng.µL^{-1}. Mobility ranges used for each targeted analysis can be found in Figures S1 and S2.*

Figure 3: Extracted ion mobility spectra of different ionic species for each HMO isomer pair as (A, B, C and D) native and (E, F, G and H) reduced forms using large mobility range detection ($1/K_0$ = 0.55-1.90 V.s.cm^{-2}). *HMOs were analyzed at 1 ng.µL^{-1} as native forms and were specifically diluted after the reduction step. In D) and H) the results were obtained for positive ESI mode after addition of lithium at 1 ng.µL^{-1}. The dilution factor for each compound analysis can be found in Figures S1-S3.*

Figure 4: IM-MS and MS/MS analyses of a breastmilk sample (1:5000 dilution in ACN/H_2O) in negative ESI mode. A) Mass spectrum showing some low abundant ions annotated as native HMO species, confirmed by, in B), their extracted ion mobility spectra as $[M+Cl]^-$, $[M+HCOO]^-$ and $[M-H]^-$ species detected both in the HMO standard mixture (1ng.µL^{-1} final concentration) and in the diluted breastmilk sample. For $[M-H]^-$ ions of the 3'SL/6'SL pair, a targeted analysis was conducted and MS/MS spectra at 45 eV extracted from their respective mobility peaks in the breastmilk sample are reported (see Figure S6 for MS/MS spectra of the standard compounds). For $[M-H]^-$ of LNFP I and LNFP V, MS/MS spectra at 15 eV are reported for the two isomers standards and for the single mobility peak (as B peak) detected in breastmilk. *Peaks labelled with *: not separated isomers, Δ: mobility peak from an isobaric compound; note that large differences in intensity detected in the mobility peaks between the standard mixtures and the breastmilk sample are highlighted by gray bands.*

Table 1

Ion species	LNT/LNnT	LNFP I/LNFP V	2'FL/3FL	3'SL/6'SL
$[M-H]^-$	**5.8%**[(a) (c)] (6.1%-7.1%)	**5.3%** [(a) (c)] (5.3%)	**1.1%** [(a) (d)] (1.0%)	**1.0%**[(e)] (0.1% - 2.1%)
$[M+Cl]^-$	**2.0%** (1.7%)	**1.7%** [(a) (c)] (1.7%)	**1.7%** [(a)] (1.8% - 3.7%)	n.d.
$[M+HCOO]^-$	**1.5%** (1.1% - 2.6%)	**4.5%** [(a)] (2.5%-4.5%)	**1.1%** (1.1% - 3.0%)	n.d.
$[M+H]^+$	**3.9%** (3.9% - 4.9%)	**5.2%** (2.3% - 5.3%)	n.d.	**3.8%** [(a) (d)] (3.8%)
$[M+Ca]^{2+}$	**3.8%** [(b) (d) (e)] (3.8%)	**1.8%** (0.5% - 2.0%)	**6.1%** [(a) (d) (e)] (4.9% - 6.8%)	**3.7%**[(b) (e)] (3.7%)
$[M+Na]^+$	**0.9%**[(b)] (0.6% - 1.2%)	**1.4%** [(a)] (1.4% - 2.6%)	**1.6%** [(a)] (1.8%)	**1.2%** (1.2%)
$[M+Li]^+$ [(f)]	**1.3%**[(a)] (0.4% - 3.0%)	**0.3%**[(a)] (0.1% - 2.3%)	**2.6%** (2.3%-2.8%)	**2.5%** (0.2% - 2.7 %)
$[M+2Li]^{2+}$ [(f)]	**2.5%** (2.6%)	**5.5%** (5.4% - 6.3%)	n.d.	n.d.

	separation using fingerprinting mode
	isomer distinction in fingerprinting mode and separation in targeted mode
	separation only in targeted mode
	no mobility separation

n.d.: not detected

Note that ΔCCS% values are reported for the major peaks when multiple peaks are detected (labelled as (a)), with few exceptions (labelled as (b)) when the largest mobility difference was obtained from minor mobility signals. In bracket, ΔCCS% values recorded in narrow mobility range detection (targeted analysis) are reported with calculated minimum and maximum ΔCCS% values when multiple mobility peaks appear under targeted analysis.

(a) ΔCCS% values between two major mobility peaks in the presence of multiple peaks for one or both isomer ions.

(b) ΔCCS% values between a major peak and a non-major peak, i.e. mobility peaks at 86%, 46% and 79% of relative intensity are considered for the $[M+HCOO]^-$ species from LNFP V, for the $[M+Ca]^{2+}$ adducts from LNnT and the $[M+Na]^+$ from LNT, respectively.

(c) Separation between two major peaks of each isomer but with overlap of a minor peak for an HMO isomer.

(d) Very high MS response of an isomer (2'FL for $[M-H]^-$, 6'SL for $[M+H]^+$, LNT and 3FL for $[M+Ca]^{2+}$ ions) hinders detection of its respective isomer (3FL for $[M-H]^-$, 3'SL for $[M+H]^+$, LNnT and 2'FL for $[M+Ca]^{2+}$) in a mixture.

(e) *The detection of a single peak reflects the presence of LNT, 3FL or 3'SL for the calcium adducts while the observation of two peaks (or more) is characteristic of the presence of LNnT, 2FL or 6'SL but does not allow to confirm the presence or the absence of their respective isomers, LNT, 3FL or 3'SL.*

(f) *The $[M+Li]^+$ and $[M+2Li]^{2+}$ adducts are formed by addition of lithium.*

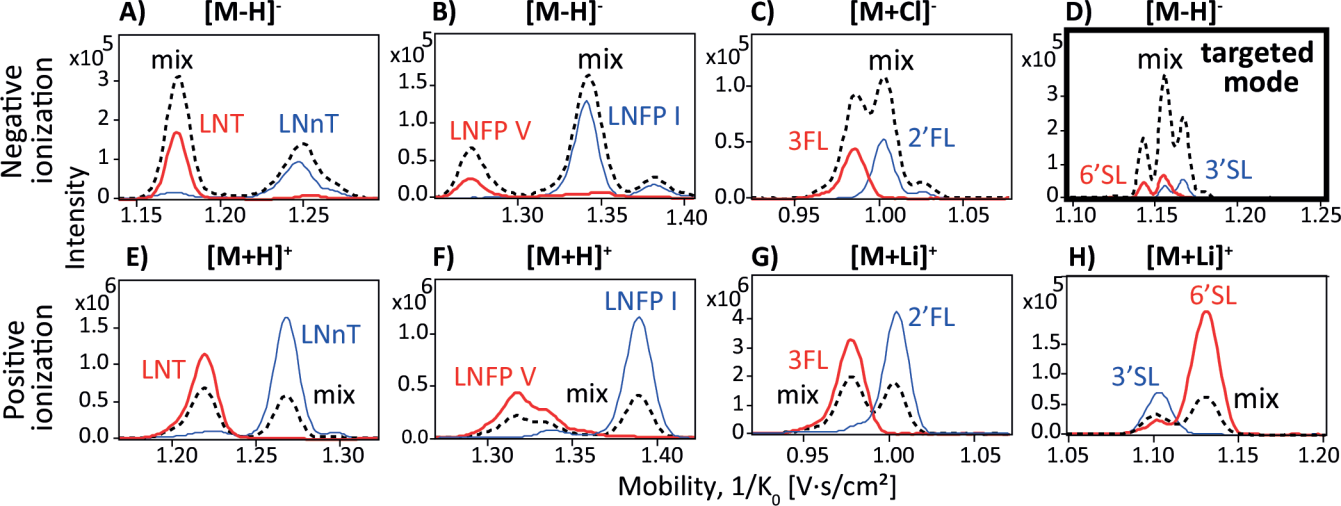
A) [M-H]⁻
B) [M-H]⁻
C) [M+Cl]⁻
D) [M-H]⁻
E) [M+H]⁺
F) [M+H]⁺
G) [M+Li]⁺
H) [M+Li]⁺
Negative ionization
Positive ionization
Intensity
mix
LNT
LNnT
LNFP V
LNFP I
3FL
2'FL
6'SL
3'SL
targeted mode
Mobility, 1/K0 [V·s/cm²]

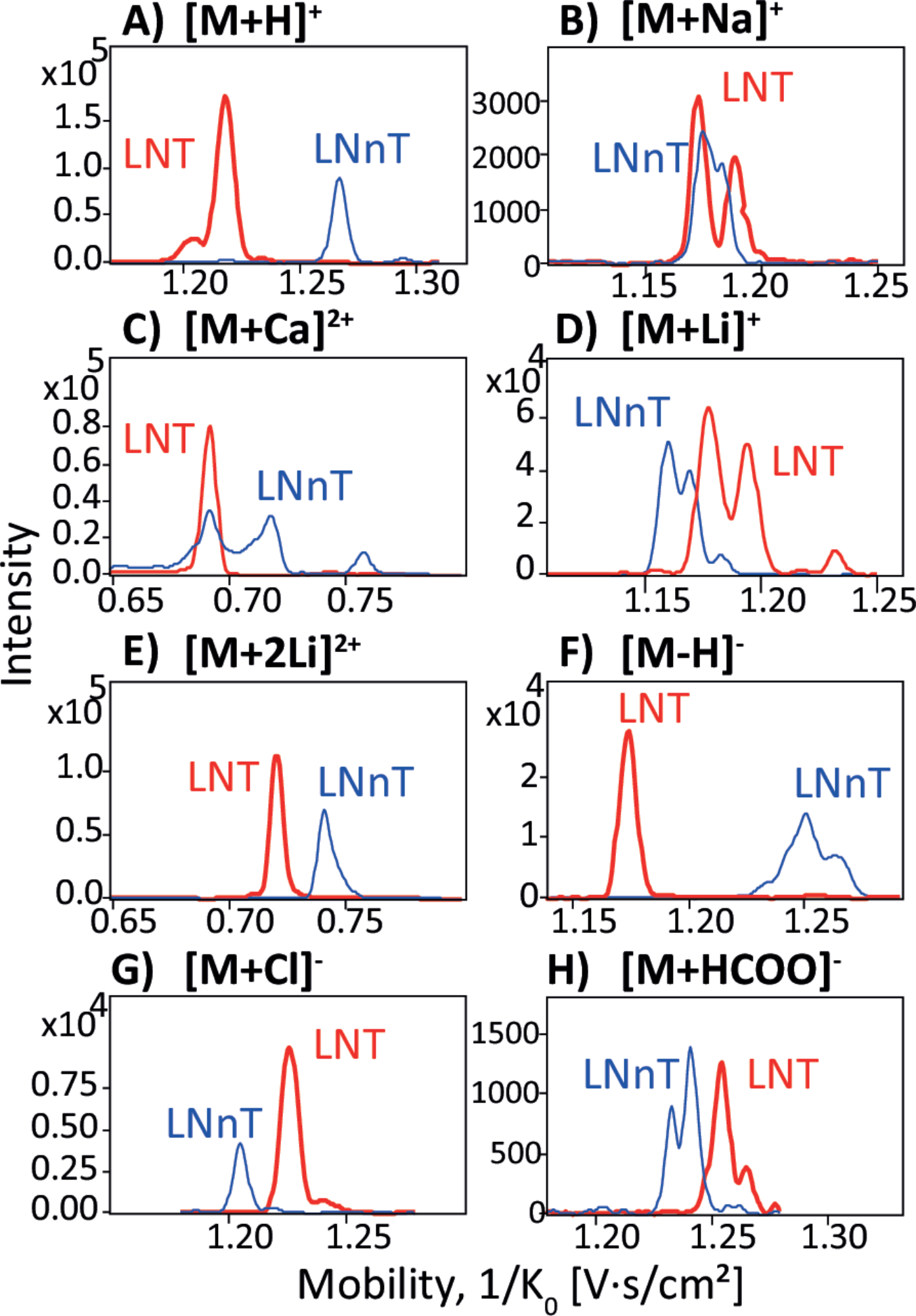
A) [M+H]+
x10 5
1.5
1.0
0.5
0.0
LNT
LNnT
1.20
1.25
1.30
B) [M+Na]+
3000
2000
1000
0
LNT
LNnT
1.15
1.20
1.25
C) [M+Ca]2+
x10 5
0.8
0.6
0.4
0.2
0.0
LNT
LNnT
0.65
0.70
0.75
D) [M+Li]+
x10 4
6
4
2
0
LNnT
LNT
1.15
1.20
1.25
Intensity
E) [M+2Li]2+
x10 5
1.0
0.5
0.0
LNT
LNnT
0.65
0.70
0.75
F) [M-H]-
x10 4
2
1
0
LNT
LNnT
1.15
1.20
1.25
G) [M+Cl]-
x10 4
0.75
0.50
0.25
0.00
LNT
LNnT
1.20
1.25
H) [M+HCOO]-
1500
1000
500
0
LNnT
LNT
1.20
1.25
1.30
Mobility, 1/K0 [V·s/cm²]

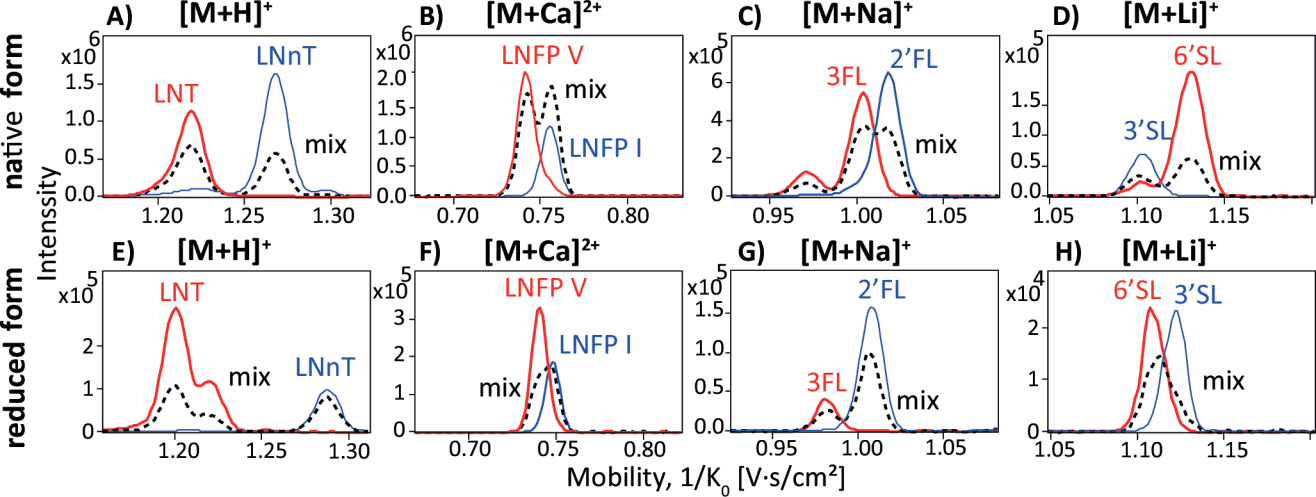
native form
reduced form
Intenssity
A) [M+H]+
B) [M+Ca]2+
C) [M+Na]+
D) [M+Li]+
E) [M+H]+
F) [M+Ca]2+
G) [M+Na]+
H) [M+Li]+
LNT
LNnT
mix
LNFP V
LNFP I
3FL
2'FL
6'SL
3'SL
Mobility, 1/K0 [V·s/cm2]

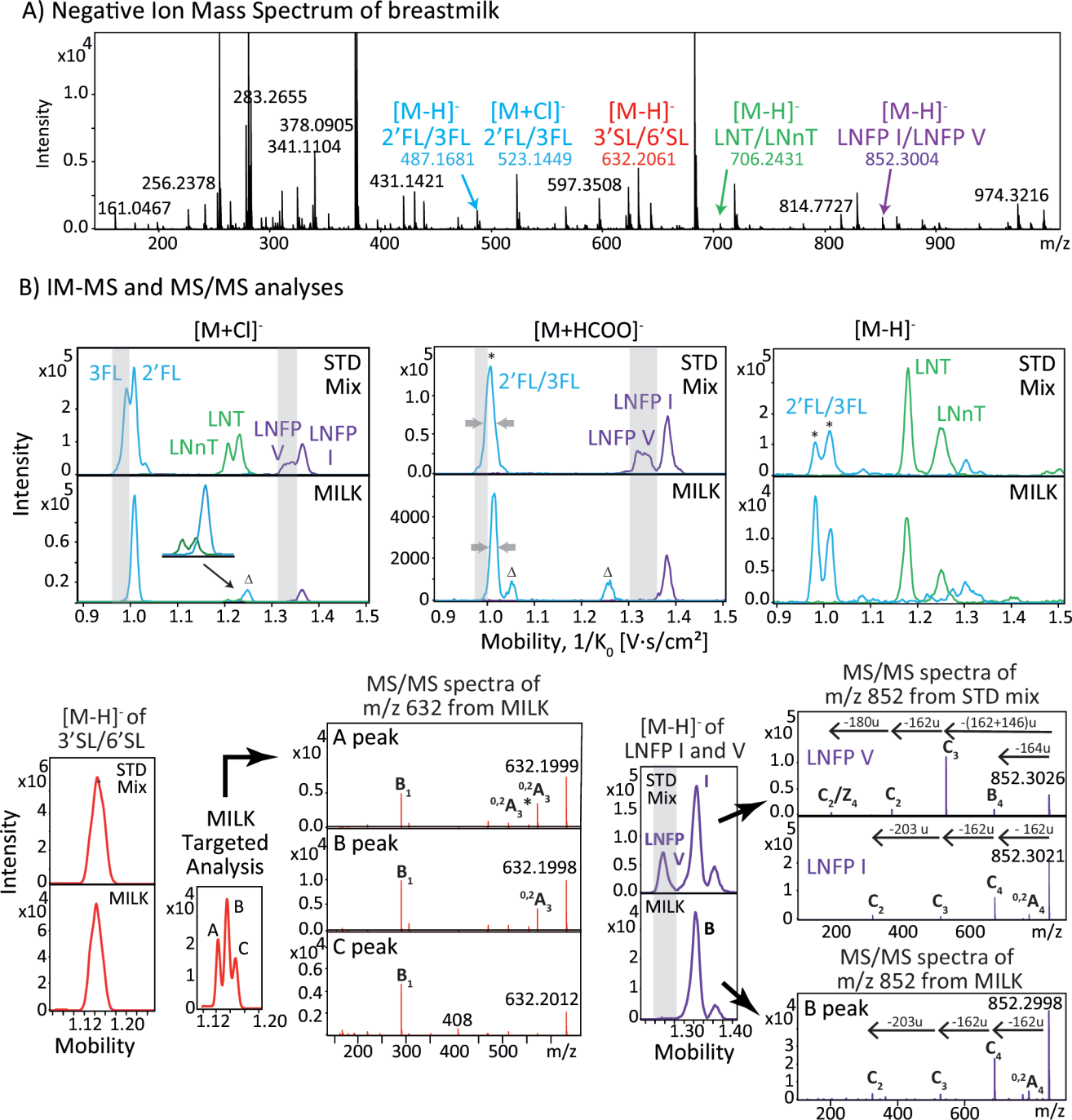
A) Negative Ion Mass Spectrum of breastmilk
Intensity
x10^4
283.2655
378.0905
341.1104
256.2378
161.0467
431.1421
[M-H]- 2'FL/3FL 487.1681
[M+Cl]- 2'FL/3FL 523.1449
[M-H]- 3'SL/6'SL 632.2061
597.3508
[M-H]- LNT/LNnT 706.2431
814.7727
[M-H]- LNFP I/LNFP V 852.3004
974.3216
m/z
B) IM-MS and MS/MS analyses
[M+Cl]-
[M+HCOO]-
[M-H]-
STD Mix
MILK
3FL
2'FL
LNT
LNnT
LNFP V
LNFP I
2'FL/3FL
Intensity
Mobility, 1/K0 [V·s/cm²]
[M-H]- of 3'SL/6'SL
MILK Targeted Analysis
MS/MS spectra of m/z 632 from MILK
A peak
B peak
C peak
632.1999
632.1998
632.2012
408
Mobility
[M-H]- of LNFP I and V
MS/MS spectra of m/z 852 from STD mix
MS/MS spectra of m/z 852 from MILK
852.3026
852.3021
852.2998
-180u
-162u
-(162+146)u
-164u
-203 u
- 162u
-203u
m/z

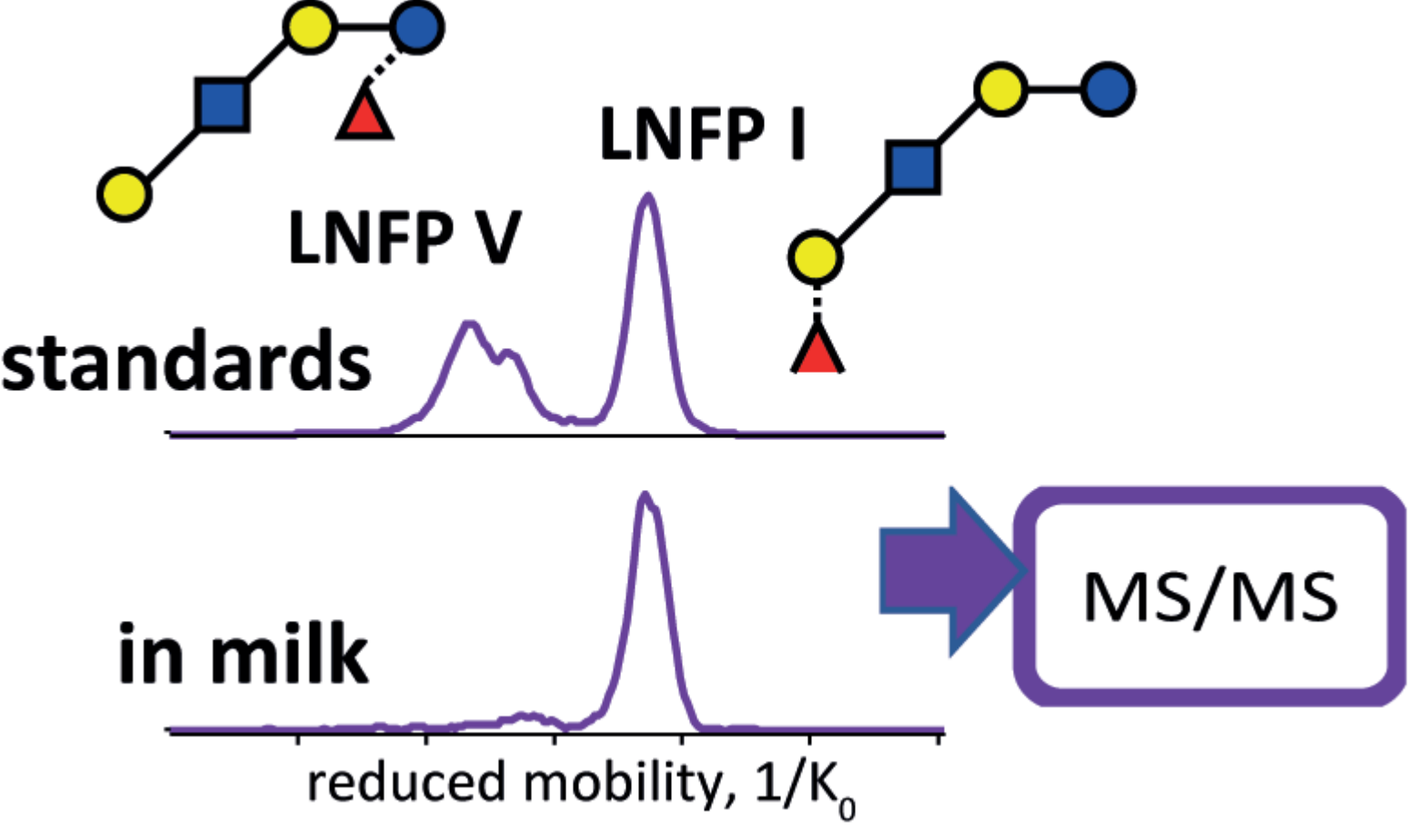
LNFP I
LNFP V
standards
in milk
MS/MS
reduced mobility, 1/K0